

# On the mechanism of carbonylation in acetic acid and higher acid synthesis from methanol and syngas mixtures on supported rhodium catalysts.

L. Chateau <sup>a</sup>, J.P. Hindermann <sup>a</sup>, A. Kiennemann <sup>a,\*</sup>, E. Tempesti <sup>b</sup>

<sup>a</sup> LERCSI-EHICS-URA CNRS 1498, 1, rue Blaise Pascal, 67000 Strasbourg, France

<sup>b</sup> Univ. Brescia, Dept. Ingegneria Meccanica, Via Valotti, 25060 Brescia, Italy

## Abstract

In high pressure gas phase conditions, methanol and syngas mixtures can be converted to acetic and higher carboxylic (C<sub>3</sub>–C<sub>5</sub>) acids on supported rhodium catalysts in presence of methyl iodide. Chemical trapping and FTIR spectroscopic studies show that two mechanisms are involved in the carboxylic acid formation. One is the conventional carbon monoxide insertion model on the rhodium part of the catalyst. The second proceeds through the isomerization of methyl formate on the support. On the support alone the chain growth stops at the C<sub>2</sub>-intermediate since no rhodium is present to convert acetic acid or methyl acetate to ethanol or ethoxy species.

**Keywords:** Methanol; Carbonylation; Acetic acid; Carboxylic acids; Rhodium catalysts; Mechanism

## 1. Introduction

Carbonylation of methanol to acetic acid is a well known industrial process. It is performed in homogeneous systems mainly by the so-called Monsanto process in presence of rhodium based catalysts at moderate temperature and pressure (150–200°C, 30–60 bar) [1]. Acetic acid can also be produced directly from CO + H<sub>2</sub> on Ru [2], Co [2] or Rh [3] containing catalysts. It has also been shown that C<sub>n</sub>H<sub>2n+1</sub>OH alcohols can be converted into C<sub>n</sub>H<sub>2n+1</sub>COOH carboxylic acids [4]. Further acetic acid can be produced by catalytic isomerization of methyl formate with Rh, Ir, Ru, Co [5] and Ni [6] catalysts. Higher monocarboxylic acids can be prepared by reacting C<sub>1–9</sub> alkyl

formates and CO + H<sub>2</sub>O in the presence of a group VIII metal compound and an iodine or bromine-containing promoter [7]. C<sub>1</sub> to C<sub>3</sub> aliphatic carboxylic acids are produced in presence of hafnium compounds from CO + H<sub>2</sub> [8]. Recently it has also been claimed that the reaction of methanol with a CO + H<sub>2</sub> mixture in presence of methyl iodide and heterogeneous supported catalysts can lead to a series of straight chain higher carboxylic acids [9,10]. The present work will be devoted to the formation of acetic acid and higher carboxylic acids on supported rhodium catalysts. Infrared spectroscopy and chemical trapping have been used to study the individual steps of carboxylic acid formation from methanol and CO + H<sub>2</sub>.

\* Corresponding author.

## 2. Experimental

### 2.1. Catalyst preparation

The rare earth oxides ( $\text{CeO}_2$ ,  $\text{Pr}_6\text{O}_{11}$ ,  $\text{La}_2\text{O}_3$ ) were prepared from their nitrate ( $\text{Ln}(\text{NO}_3)_3 \cdot 6\text{H}_2\text{O}$ ; Ln = rare earth). 10 g  $\text{Ln}(\text{NO}_3)_3 \cdot 6\text{H}_2\text{O}$  were dissolved in 400 ml distilled water, heated under stirring at  $80^\circ\text{C}$ . The pH was adjusted to 7 with ammonia. The precipitate was filtered, washed, dried at  $120^\circ\text{C}$  and calcined in air at  $400^\circ\text{C}$  for 10 h.  $\text{ZrO}_2$  was prepared by hydrolysis of  $\text{Zr}(\text{C}_3\text{H}_7\text{O})_4$  (Fluka). The pH was adjusted to 7 by ammonia, and the precipitate was treated like that of rare earths.  $\text{SiO}_2$  has been purchased from Degussa (Sipernat 22). The  $\text{La}_2\text{Zr}_2\text{O}_7$  pyrochlore has been prepared as follows. The precursors ( $\text{La}(\text{NO}_3)_3 \cdot 6\text{H}_2\text{O}$  and  $\text{Zr}(\text{C}_3\text{H}_7\text{O})_4$ ) are dissolved in alcohol, precipitated by oxalic acid, filtered and calcined at  $700^\circ\text{C}$ . The BET specific surface area of the oxides were about  $35 \text{ m}^2 \text{ g}^{-1}$ .

The catalysts were prepared by a conventional impregnation of the support by the suitable amount of an aqueous solution of  $\text{RhCl}_3 \cdot x\text{H}_2\text{O}$  from Johnson Matthey to obtain 3 wt%Rh/support. The catalysts were dried at  $120^\circ\text{C}$  and calcined in air at  $450^\circ\text{C}$  for 10 h.

### 2.2. Activity measurements

The catalytic tests have been performed in a stainless steel (Z2CND17-12) reactor of 8 mm inner diameter which has been lined by a copper tube of 6 mm inner diameter. The length of the heated part was 0.43 m and the catalyst was maintained in the middle part of the reactor by glass wool plugs. The  $\text{CO-H}_2$  mixture has been prepared in the laboratory and controlled by GC with a TCD detector. The synthesis gas was then compressed to 50 MPa in a 500 ml high pressure vessel. The pressure in the device (21 MPa) is regulated by a Tescom 70 MPA, the gas flow is measured by a Setaram 3100 flowmeter and regulated by an electronic controller coupled with a Brooks 5835N electrovalve. At the exit of the

reactor the liquids are trapped at  $10^\circ\text{C}$  under high pressure. The pressure of the exit gas is reduced to 2 MPa and analyzed by GC with both TCD and FID detectors. The  $\text{CH}_3\text{OH-CH}_3\text{I}$  mixture is cooled to  $0^\circ\text{C}$  to avoid evaporation and introduced into the device by a model 303 Gilson metering pump. Previous to the catalytic test, the catalyst (0.5 g) is reduced by hydrogen at  $230^\circ\text{C}$  during 15 h. The hydrogen is then released and the synthesis gas is progressively introduced. The samples are collected after 24 h in order to achieve the steady state.

### 2.3. FTIR spectroscopy

10 to 20 mg of catalyst were pelleted as a disk 12 mm in diameter. The spectra were taken in a vacuum device similar to that used by Lamotte [11]. The spectra were recorded on a Nicolet MX1 FTIR spectrometer after 100 scans with a  $4 \text{ cm}^{-1}$  resolution. The catalysts are reduced in situ at  $400^\circ\text{C}$  by hydrogen which has been admitted into the cell. The hydrogen atmosphere was then pumped off and the procedure was repeated 5 times. Metal particle size as measured by carbon monoxide adsorption by pulse techniques were estimated to be 2.5 nm for Rh/ $\text{CeO}_2$  and 1.9 nm for Rh/ $\text{Pr}_6\text{O}_{11}$ . 3 to 5 kPa of products were introduced into the vacuum device and the first spectrum was taken after 5 min at room temperature. The pellet was then lifted into the heating part for 10 min. The pellet was reintroduced into the beam at room temperature, the pressure being maintained constant during the measurement. The reported spectra are obtained after subtraction of the catalytic pellet and the gas phase spectra.

### 2.4. Chemical trapping experiments

The device used for the chemical trapping has been reported elsewhere [12]. The species were trapped at  $120^\circ\text{C}$  by an excess of  $\text{CH}_3\text{I}$  or  $\text{CD}_3\text{I}$ .

### 3. Results and discussion

#### 3.1. Activity measurements

The results obtained in continuous flow experiments at the steady state are given in Table 1.

It can be seen that almost all tested catalysts give a chain growth in our reaction conditions. Rh/La<sub>2</sub>O<sub>3</sub> has the best productivity, however rhodium is rapidly lost from the catalytic surface and lanthanum is dissolved as lanthanum acetate. The selectivity for methyl acetate is much higher on the Rh/CeO<sub>2</sub> catalyst which gives no further chain growth. In order to control if acetic acid is an intermediate in the C<sub>3</sub> acid formation, acetic acid was introduced with a CO + H<sub>2</sub> flow into the reactor. The obtained results are given in Table 2.

It can be seen that acetic acid takes part in the chain growth but that its reduction to ethanol or ethoxy species is rate determining since in the same conditions ethanol is almost completely converted to propionic acid with a good selectivity.

Thus from these experiments it can be proposed that the reaction sequence is the following:

CH<sub>3</sub>OH

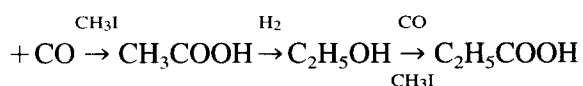


Table 2  
Acetic acid ethanol carbonylation

Catalyst	Remaining reagent %	Selectivity %						
		Acids						
		CH <sub>3</sub> OH	AcMe	AcEt	C <sub>2</sub>	C <sub>3</sub>	C <sub>4</sub>	C <sub>5</sub>
5%Rh/La <sub>2</sub> O <sub>3</sub>	88.7 <sup>a</sup>	26.3	7.4	4.1	–	60.1	2.1	–
5%Rh/La <sub>2</sub> O <sub>3</sub>	13.1 <sup>b</sup>	–	4.7	7.1	11.8	63.3	4.5	0.2

<sup>a</sup> Acetic acid.

<sup>b</sup> Ethanol.

Operating conditions see Table 1.

#### 3.2. Carbon monoxide adsorption

The attribution of bands in the FTIR spectra of carbon monoxide adsorbed on 3%Rh/Pr<sub>6</sub>O<sub>11</sub> is given in Table 3. A band at 2066 cm<sup>-1</sup> can be attributed to a linearly adsorbed species. Two small ones at 1908 and 1882 correspond to carbon monoxide chemisorbed in a bridging configuration. According to the literature the band at 1908 cm<sup>-1</sup> has been ascribed to CO bridge bonded to two rhodium atoms on the rhodium (100) face [13]. It shifts to 1944 cm<sup>-1</sup> for higher coverages. The band at 1882 cm<sup>-1</sup> arises from CO adsorption on the more dense (111) face. Similar observations have been made for rhodium supported on CeO<sub>2</sub> [14,15]. It seems that this could point to a dependence of the activity from the morphology of the rhodium particle [16]. Further a low frequency band appears at 1720 cm<sup>-1</sup>. It corresponds

Table 1  
Activity test

Catalyst	CH <sub>3</sub> OH remaining (%)	Selectivity %			Acids			Productivity g · g cat <sup>-1</sup> · h <sup>-1</sup>
		AcMe	AcEt	AcPr	C <sub>2</sub>	C <sub>3</sub>	C <sub>4</sub>	
3%Rh/Pr <sub>6</sub> O <sub>11</sub>	33	6.3	1.4	–	87.7	4.6	–	0.2
3%Rh/La <sub>2</sub> O <sub>3</sub>	3.7	1.9	1.9	–	91.9	5.1	–	1.2
5%Rh/CeO <sub>2</sub>	26.6	54.3	0.3	–	45.4	–	–	0.2
5%Rh/ZrO <sub>2</sub>	4.4	2.5	2.7	0.3	85.5	8.6	0.4	0.7
5%Rh/La <sub>2</sub> Zr <sub>2</sub> O <sub>7</sub>	0.8	0.7	1.8	–	94.8	2.7	–	0.7
3%Rh/SiO <sub>2</sub>	49.4	3.7	1.2	–	81.7	12.8	–	0.6

Operating conditions:  $P = 21$  MPa,  $T = 230^\circ\text{C}$ ,  $\text{CO}/\text{H}_2 = 60/40$ , gas flow =  $3 \text{ l} \cdot \text{h}^{-1} \cdot \text{g cat}^{-1}$ ,  $\text{MeOH}/\text{CH}_3\text{I} = 7.7/1$  molar,  $\text{CH}_3\text{OH} + \text{CH}_3\text{I}$  flow =  $0.2 \text{ ml} \cdot \text{h}^{-1} \cdot \text{g cat}^{-1}$ .

Table 3  
CO stretching frequencies ( $\text{cm}^{-1}$ ) and attribution to adsorbed  $^{12}\text{C}^{16}\text{O}$ ,  $^{13}\text{C}^{16}\text{O}$  and  $^{12}\text{C}^{18}\text{O}$  in the FTIR spectra

Adsorbed species	Linear	Bridged	C–O bonded	gem. dicarbonyl
$^{12}\text{C}^{16}\text{O}$				
3%Rh–Pr <sub>6</sub> O <sub>11</sub>	2066	1908, 1882	1720	2096, 2029
Rh–Mn/SiO <sub>2</sub> (24)	2055	1815	1713	
$^{13}\text{C}^{16}\text{O}$				
Rh/Pr <sub>6</sub> O <sub>11</sub>	1990	1848, 1778	1638	2008, 1956
Rh–Mn/SiO <sub>2</sub> (24)	2012	1770	1670	
$^{12}\text{C}^{18}\text{O}$				
Rh/Pr <sub>6</sub> O <sub>11</sub>	2012	1853, 1779	1660	2045, 1984
Rh–Mn/SiO <sub>2</sub> (24)	2010	1797	~1700	

to that observed on a Rh–CeO<sub>2</sub>/SiO<sub>2</sub> catalyst [14]. This low frequency feature has been attributed to a carbon monoxide species which is coordinated to the surface both through carbon and

oxygen [14,17–20]. At room temperature twin bands are observed at 2096 and 2029  $\text{cm}^{-1}$  and can be attributed to the symmetric and antisymmetric vibrations of gem carbonyl species on isolated Rh<sup>1+</sup> sites [17–20] resulting from the rupture of Rh–Rh bonds in small particles [19,21–23]. In order to confirm the attribution of the bands,  $^{13}\text{C}^{16}\text{O}$  and  $^{12}\text{C}^{18}\text{O}$  have been adsorbed on 3%Rh/Pr<sub>6</sub>O<sub>11</sub> (Table 3) and the results are compared to that of Ichikawa et al. [24] on Rh–Mn/SiO<sub>2</sub>.

Very similar results are thus obtained on Rh/Pr<sub>6</sub>O<sub>11</sub> and Rh–Mn/SiO<sub>2</sub>, except that for  $^{12}\text{C}^{18}\text{O}$  adsorption, the expected shift in the C and O bonded species ( $\sim 60 \text{ cm}^{-1}$ ) is present, whereas Ichikawa et al. [24] observed that the position of this low frequency band is very near to that observed for  $^{12}\text{C}^{16}\text{O}$  suggesting that on Rh–Mn/SiO<sub>2</sub> a facile  $^{18}\text{O}$  to  $^{16}\text{O}$  exchange occurs. By heating, the linear and bridge bonded species are more rapidly desorbed than the C and O bonded species.

Table 4  
FTIR spectra of adsorbed methanol and attribution of bands (25). In brackets deuterated compounds

Catalyst Species	SiO <sub>2</sub>	Rh/SiO <sub>2</sub>	CeO <sub>2</sub>	Rh/CeO <sub>2</sub>	Pr <sub>6</sub> O <sub>11</sub>	Rh/Pr <sub>6</sub> O <sub>11</sub>
Methoxy/Rh						
$\nu\text{sCH}_3$				2950		2950
$\nu\text{C–O}$				1023		1028
Methoxy/Support						
$\nu\text{aCH}_3$	3006	3006				
$\nu\text{aCH}_3$	2950	2950(2243)	2921(2162)	2931	2926	2931(2176)
Fermi resonance						
$2\delta\text{CH}_3 + \nu\text{sCH}_3$			2856	2856	2846	2846
$\nu\text{sCH}_3$	2850	2850(2142)	2790	2804	2790	2806(2078)
$\delta\text{aCH}_3$	1470	1470	(1131)			1468(1121)
$\delta\text{sCH}_3$	1457	1457	1459(1051)	1454	1431	
$\nu\text{C–O}$			1076(1018)	1070	1065	1060(1070)
Formyl				2770		2737(1960)
$\nu\text{CH}$				2660		2660
				2596		
$\nu\text{C=O}$				1665		1665(1656)
Adsorbed CO						
linear		2052		2039		2012
bridged		1900		1848		
Formate						
$\nu\text{CH}$			2878(2120)	2879	2878	2879(2134)
$\nu\text{a(OCO)}$			1571(1567)	1572	1595	1581(1554)
$\nu\text{s(OCO)}$			1370(1370)	1375	1351	1370(1370)

This indicate a stronger bonding of the latter to the catalytic surface.

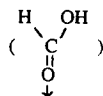
### 3.3. Methanol and formaldehyde adsorption

The FTIR spectra of adsorbed methanol and formaldehyde have been interpreted and published elsewhere for Rh/SiO<sub>2</sub> and Rh/CeO<sub>2</sub> [25]. The results are summarized in Table 4 and Table 5, respectively, and compared to that obtained on Rh/Pr<sub>6</sub>O<sub>11</sub> in the present work. The most striking result is the formation of formyl species on the CeO<sub>2</sub> and Pr<sub>6</sub>O<sub>11</sub> supported rhodium catalysts. It seems that one of the roles of the support is to stabilize these formyl species when compared to a silica supported catalyst.

### 3.4. Adsorption of formic acid

FTIR spectra of formic acid on Pr<sub>6</sub>O<sub>11</sub> are given on Fig. 1. A band at 2940 cm<sup>-1</sup> could correspond to physisorbed formic acid [26]. Bands at 2855 and 1696 cm<sup>-1</sup> are similar to that observed by Millar et al. [26] on supported copper catalysts.

These authors attribute these features to  $\nu\text{CH}$  and  $\nu\text{C}=\text{O}$  of formic acid coordinated by oxygen to a Lewis acid site



The band at 1696 cm<sup>-1</sup> disappears upon heating. Two bands at 1565 and 1536 cm<sup>-1</sup> could be attributed to the  $\nu\text{a}(\text{OCO})$  vibrations of bidentate formates adsorbed on two different sites. They correspond to  $\nu\text{s}(\text{OCO})$  features at 1335 and 1373 cm<sup>-1</sup> and to a  $\delta(\text{OCO})$  vibration at 773 cm<sup>-1</sup>. These bands can be ascribed by comparison with the results of Li et al. on CeO<sub>2</sub> [27]. Two types of monodentate formates have also been evidenced with  $\nu\text{a}(\text{OCO})$  at 1604 and 1590 cm<sup>-1</sup> and  $\nu\text{s}(\text{OCO})$  at 1270 cm<sup>-1</sup>. Bands observed at 1066, 1175, 1467 and 1476 cm<sup>-1</sup> are similar to that obtained by CH<sub>2</sub>O adsorption on TiO<sub>2</sub> and ZrO<sub>2</sub> and attributed to  $\nu\text{C}-\text{O}$ ,  $\rho\text{CH}_2$ ,  $\omega\text{CH}_2$  and  $\delta\text{CH}_2$  of a dioxymethylene species [28]. When the sample is heated to 60°C bands appear at 1507,

Table 5  
FTIR spectra of adsorbed formaldehyde and attribution of bands.

Catalyst species	Pr <sub>6</sub> O <sub>11</sub>	Rh/Pr <sub>6</sub> O <sub>11</sub>	Catalyst species	Pr <sub>6</sub> O <sub>11</sub>	Rh/Pr <sub>6</sub> O <sub>11</sub>
Methoxy/support			dioxymethylene		
$\nu\text{CH}_3$	2921	2921	$\delta\text{CH}_2$		1492
Fermi resonance			$\omega\text{CH}_2$		1407
$2\delta\text{CH}_3 + \nu\text{sCH}_3$	2850	2850	$\nu\text{CO}$		1112
$\nu\text{sCH}_3$	2800	2800	$\rho\text{CH}_2$		925
$\delta\text{sCH}_3$	1430	1430			
$\nu\text{C}-\text{O}$	1065	1065			
Formate/support			$\eta^2(\text{C},\text{O})\text{CH}_2\text{O}$		
$\nu\text{CH}$	2865	2865	$\nu\text{aCH}_2$	2940	2940
$\nu\text{a}(\text{OCO})$	1605		$\delta\text{CH}_2$	1430	1430
	(monodentate)				
$\nu\text{a}(\text{OCO})$	1565	1567	$\omega\text{CH}_2$	1159	1159
	(bidentate)		$\nu\text{C}-\text{O}$	967	967
$\nu\text{s}(\text{OCO})$	1375	1375	$\rho\text{CH}_2$	864	864
Formyl					
$\nu\text{CH}$		2762			
		2645			
		2556			
$\nu\text{CO}$		1665			

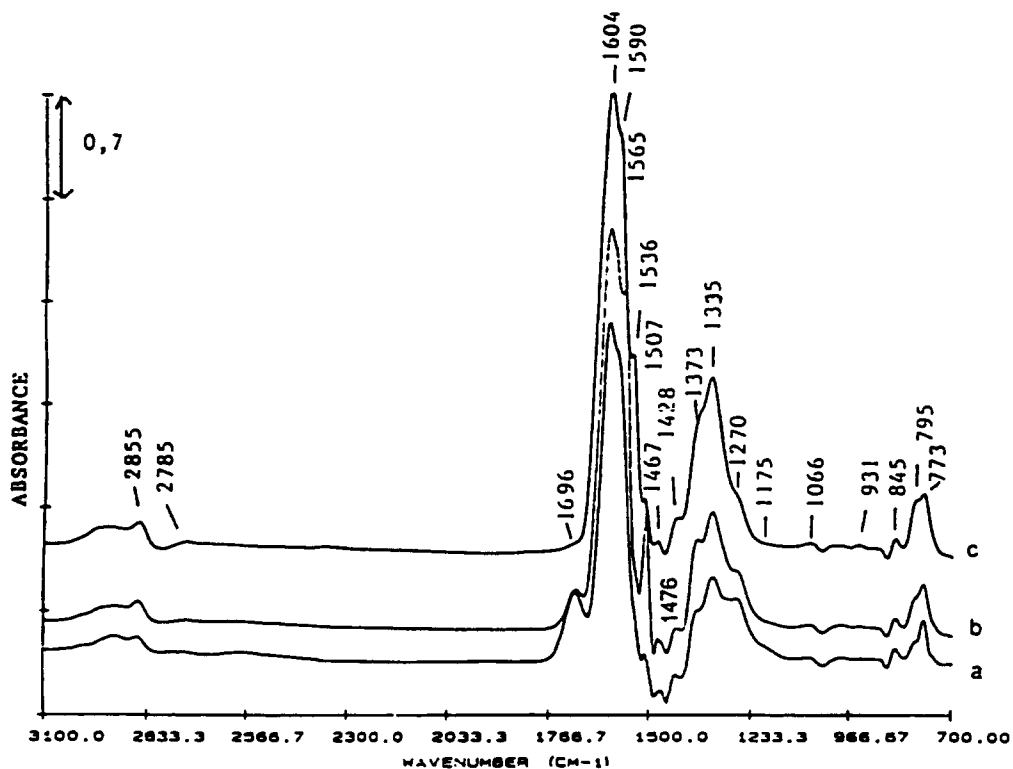


Fig. 1. FTIR spectra of formic acid adsorbed on  $\text{Pr}_6\text{O}_{11}$  (20 mbar): (a) room temperature, (b)  $60^\circ\text{C}$ , (c)  $120^\circ\text{C}$ .

$2678$  and  $2785\text{ cm}^{-1}$ , whereas the feature at  $1373\text{ cm}^{-1}$  broadens and is shifted to  $1380\text{ cm}^{-1}$ . At  $120^\circ\text{C}$  these bands disappear again. Comparing to the results obtained by Saussey et al. [29] upon adsorption of  $\text{CO} + \text{H}_2$  on  $\text{ZnO}$  ( $\delta\text{CH}$ :  $1371$ ,  $\nu\text{C}-\text{O}$ :  $1521$  and  $\nu\text{CH}$ :  $2664$  and  $2769\text{ cm}^{-1}$ ), these features could be attributed to the formation of a formyl species.

The FTIR spectra of formic acid on  $\text{Rh}/\text{Pr}_6\text{O}_{11}$  show only few differences with that of the adsorption on the support. However it seems that only one of the bidentate formate species is present ( $\nu\text{a}(\text{OCO})$ :  $1553$ ,  $\nu\text{s}(\text{OCO})$ :  $1375$  and  $\delta(\text{OCO})$ :  $765\text{ cm}^{-1}$ ).

At  $789\text{ cm}^{-1}$ , there is a feature which does not appear on the support alone. Lamotte [11] has evidenced a band in the same area on  $\text{Cu}/\text{ZnO}$  and suggested that it might be ascribed to the formation of a formic anhydride adsorbed on the surface. The band at  $1507\text{ cm}^{-1}$  on the support alone is shifted to  $1529\text{ cm}^{-1}$  and can also be attributed to a formyl species.

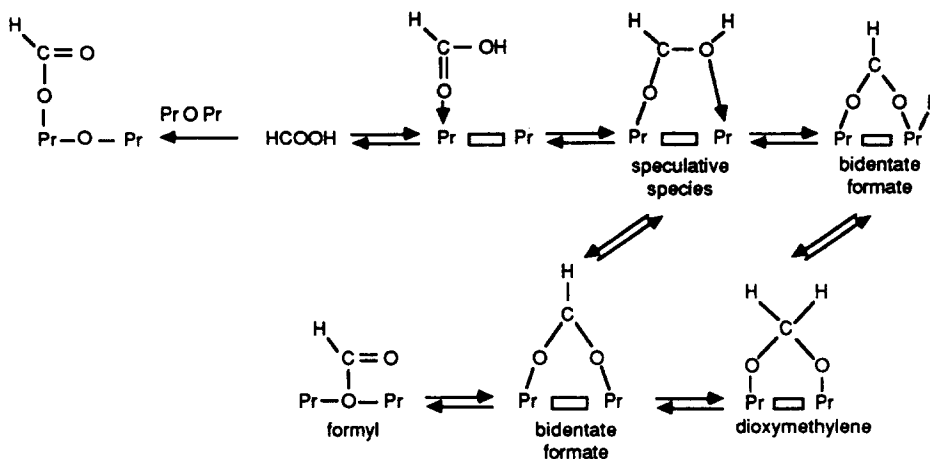
The presence of different formate species on the support can be explained by the fact that  $\text{Pr}_6\text{O}_{11}$  is partially reduced to  $\text{Pr}_2\text{O}_3$  and that the charge of Pr is somewhere between  $3(\text{Pr}_2\text{O}_3)$  and  $3.66(\text{Pr}_6\text{O}_{11})$  and therefore several different adsorption sites may be present. In presence of rhodium, more activated hydrogen can be provided to the support and only one adsorption site remains. The results obtained for the adsorption on the catalyst suggest that the reactions outlined in Scheme 1 might be operative.



species have previously been proposed by Hattori and Wang to be present on the surface of  $\text{MgO}$  [30] after interaction with  $\text{CO} + \text{H}_2$ .

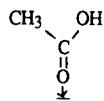
### 3.5. Adsorption of acetic acid

Acetic acid was adsorbed on  $\text{Pr}_6\text{O}_{11}$  at room temperature (Fig. 2). The stretching frequencies

Scheme 1. Evolution of formic acid chemisorbed on  $\text{Pr}_6\text{O}_{11}$ .

of  $\text{CH}_3$  of acetate were observed at 3023, 2997 ( $\nu\text{aCH}_3$ ) and 2940  $\text{cm}^{-1}$  ( $\nu\text{sCH}_3$ ). The band at 1568  $\text{cm}^{-1}$  can be attributed to  $\nu\text{a}(\text{OCO})$  according to the results of Sexton [31] obtained by adsorption of acetic acid on  $\text{Cu}(100)$ , whereas the feature at 1428  $\text{cm}^{-1}$  could be ascribed to the  $\nu\text{s}(\text{OCO})$  vibration.  $\delta\text{CH}_3$  appears at 1338  $\text{cm}^{-1}$  and combination between  $\delta(\text{OCO})$  (650  $\text{cm}^{-1}$ ) and  $\rho(\text{OCO})$  (624  $\text{cm}^{-1}$ ) gives rise to a band at 1275  $\text{cm}^{-1}$ . The bands at 1055 and 1020  $\text{cm}^{-1}$  correspond to  $\rho\text{CH}_3$  and that at 935  $\text{cm}^{-1}$  to the  $\nu\text{a}(\text{C}-\text{C})$  stretching vibration [32].

At room temperature a band at 1698  $\text{cm}^{-1}$  which disappears upon heating is similar to that obtained by adsorption of formic acid and can therefore be attributed to a species adsorbed on the surface through its oxygen as follows:



The same bands are observed on  $\text{Rh}/\text{Pr}_6\text{O}_{11}$  but two features appear in the area of  $\nu\text{a}(\text{OCO})$  (1568 and 1558  $\text{cm}^{-1}$ ) and of  $\nu\text{s}(\text{OCO})$  (1453 and 1427  $\text{cm}^{-1}$ ). This corresponds to two types of acetates located one on the support and the second possibly on rhodium. The combination band between  $\delta(\text{OCO})$  and  $\rho(\text{OCO})$  is shifted to a lower frequency (1253 instead of 1277  $\text{cm}^{-1}$ ). Like on  $\text{Pr}_6\text{O}_{11}$ , a band appears at 1703  $\text{cm}^{-1}$  and

could correspond to an O adsorbed acetic acid. Indeed it disappears readily upon heating.

### 3.6. Acetaldehyde adsorption

Acetaldehyde adsorption on unpromoted and promoted ( $\text{CeO}_2$ ,  $\text{ZrO}_2$ )  $\text{Rh}/\text{SiO}_2$  has been studied and published by Demri et al. [33]. The most striking point is the stabilization of an acetyl species on the surface of the promoted catalysts. On  $\text{Rh}/\text{Pr}_6\text{O}_{11}$ , at room temperature a band at 1694  $\text{cm}^{-1}$  is characteristic of the  $\nu\text{C}=\text{O}$  vibration of physisorbed acetaldehyde [34]. A series of features can also be associated with this physisorbed species ( $\nu\text{CH}$ : 2866, combination bands: 2824, 2767,  $\delta\text{aCH}_3$ : 1440,  $\rho\text{CH}$ : 1407 and 1384,  $\delta\text{sCH}_3$ : 1342,  $\nu\text{aC}-\text{C}$ : 1127 and 1098  $\text{cm}^{-1}$ ).

By heating the sample to 120°C a new band appears at 1665  $\text{cm}^{-1}$ . This band disappears by further heating. A series of other bands appears and disappears in same time as the previous one and correspond well to the features observed by Hieber et al. [35] for an acetyl linked to a neutral rhenium carbonyl complex ( $\nu\text{CH}_3$ : 2903,  $\nu\text{aC}-\text{C}$ : 1094,  $\rho\text{CH}_3$ : 957 and 910  $\text{cm}^{-1}$ ). The similarity of the results presented here with those found by Demri et al. [33] leads us to attribute this species to a stabilized acetyl species. Further, acetate species are also observed during the heating of the sample: ( $\nu\text{aCH}_3$ : 3016, 2987,  $\nu\text{sCH}_3$ : 2940,  $\nu\text{aO}-\text{C}-\text{O}$ : 1555,  $\rho\text{CH}_3$ : 1052 and 1009  $\text{cm}^{-1}$ ).

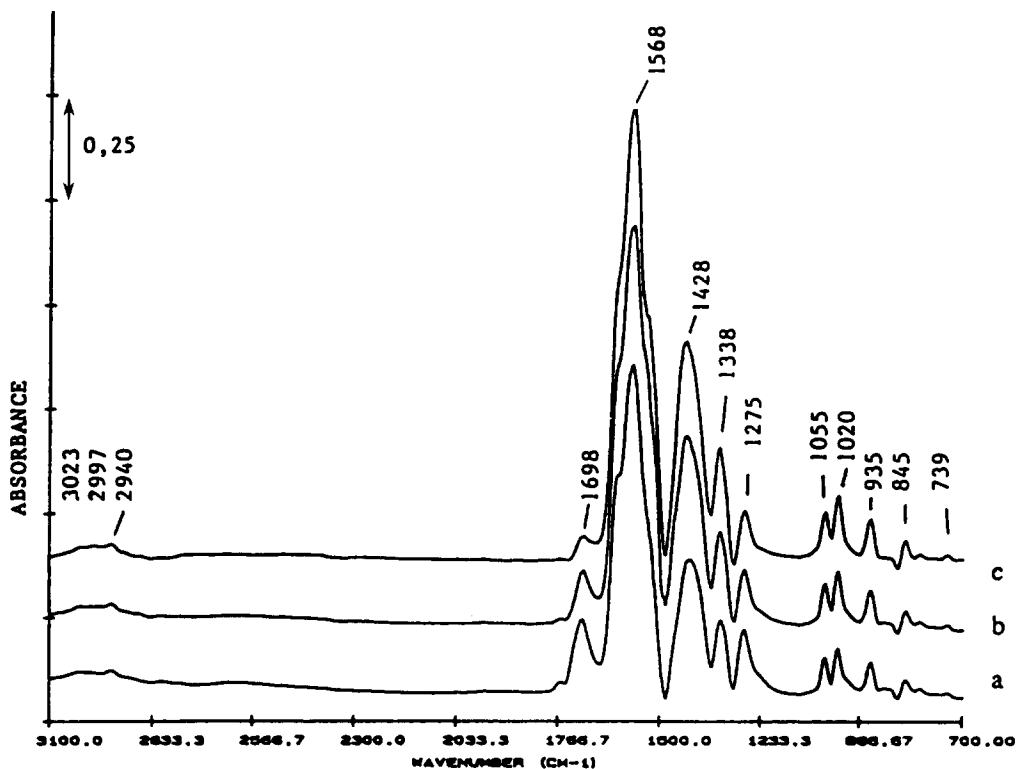


Fig. 2. FTIR spectra of acetic acid adsorbed on  $\text{Pr}_6\text{O}_{11}$  (20 mbar): (a) room temperature, (b) 60°C, (c) 120°C.

### 3.7. Surface coupling reactions

In order to elucidate the mechanism of chain growth on  $\text{Rh}/\text{Pr}_6\text{O}_{11}$ , two reactions have been studied:  $\text{CH}_3\text{I} + \text{CO}$  and  $\text{CH}_3\text{OH} + \text{CO}$ .

### 3.8. $\text{CH}_3\text{I} + \text{CO}$ (Fig. 3)

Addition of  $\text{CH}_3\text{I}$  on  $\text{Rh}/\text{Pr}_6\text{O}_{11}$  results immediately in a peak at  $1248\text{ cm}^{-1}$  which is characteristic of a chemisorbed  $\text{CH}_3$  species. Upon addition of  $\text{CO}$  the bands of chemisorbed carbon monoxide appear at  $2059\text{ cm}^{-1}$  (linear),  $2092$  and  $2036\text{ cm}^{-1}$  (gem-dicarbonyl) and  $1895$  and  $1851\text{ cm}^{-1}$  (bridged). By heating to  $90^\circ\text{C}$ , features corresponding to an acetate species develop in the spectrum ( $\nu\text{aCH}_3$ :  $3034$  and  $2979$ ,  $\nu\text{sCH}_3$ :  $2931$ ;  $\nu\text{a}(\text{OCO})$ :  $1555$ ;  $\nu\text{s}(\text{OCO})$ :  $1421$ ;  $\delta\text{CH}_3$ :  $1345$ ;  $\rho\text{CH}_3$ :  $1068$ ,  $1016$  and  $\delta\text{a}(\text{OCO})$ :  $943\text{ cm}^{-1}$ ). At the same time a band increases at  $1655\text{ cm}^{-1}$  together with features at  $2955$ ,  $2898$ ,  $1412$ ,  $1093$  and  $943\text{ cm}^{-1}$ ). If compared to the spectra of the acetyl observed by Hieber et al. [35]

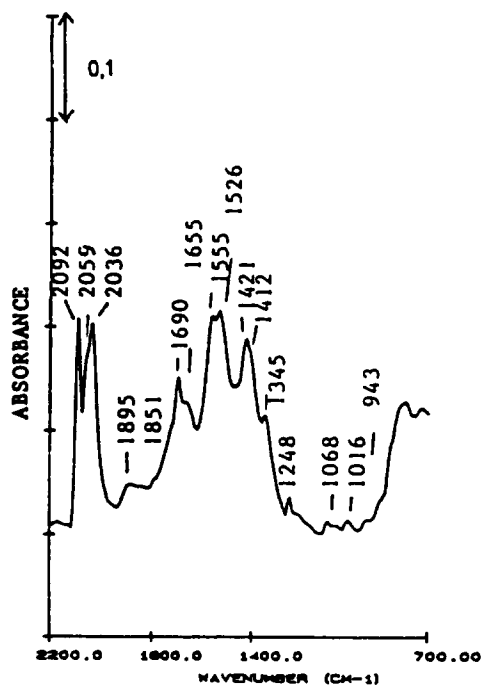


Fig. 3. FTIR spectra of  $\text{CH}_3\text{I} + \text{CO}$  adsorbed on 3%  $\text{Rh}/\text{Pr}_6\text{O}_{11}$  (20 mbar):  $T = 90^\circ\text{C}$ .



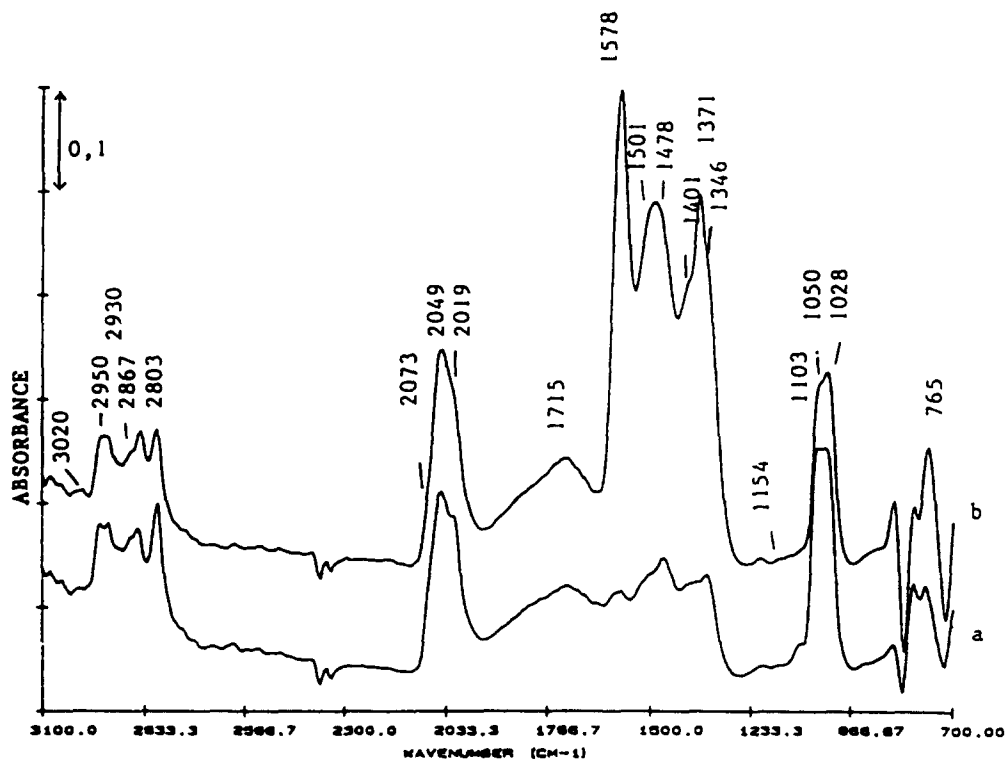


Fig. 4. FTIR spectra of  $\text{CH}_3\text{OH} + \text{CO}$  adsorbed on 3%  $\text{Rh}/\text{Pr}_6\text{O}_{11}$  (20 mbar): (a)  $60^\circ\text{C}$ , (b)  $180^\circ\text{C}$ .

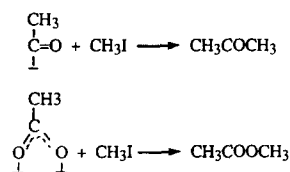
( $\nu\text{CH}_3$ : 2964, 2900;  $\nu\text{C}=\text{O}$ : 1667;  $\delta_s\text{CH}_3$ : 1409,  $\delta_a\text{C}-\text{C}$ : 1054 and  $\rho\text{CH}_3$ : 957  $\text{cm}^{-1}$ ) it can be concluded that an acetyl species is formed by the reaction of  $\text{CH}_3\text{I}$  with  $\text{CO}$  on the catalytic surface.

Adsorbed acetaldehyde can also be observed ( $\nu\text{C}=\text{O}$ : 1690,  $\delta_s\text{CH}_3$ : 1346,  $\nu\text{CH}$ : 2781  $\text{cm}^{-1}$  and a combination band at 2823  $\text{cm}^{-1}$ ). Acetaldehyde can indeed be formed by reaction of the acetyl species with adsorbed hydrogen from the catalyst's reduction.

Table 6  
Attribution of bands for  $\text{CH}_3\text{OH} + \text{CO}$  adsorption ( $\text{cm}^{-1}$ ) on  $\text{Rh}/\text{Pr}_6\text{O}_{11}$  at room temperature

linear CO	$\nu\text{CO}$	2050	methoxy on $\text{Pr}_6\text{O}_{11}$ monodentate	
gem carbonyl	$\nu\text{CO}$	2073	$2\delta\text{CH}_3 + \nu_s\text{CH}_3$	
		2019	$\nu_s(\text{C}-\text{O})$	
methoxy on Rh	$\nu_a\text{CH}_3$	3020	bidentate	
		2950	$\nu_a\text{CH}_3$	2930
	$\nu\text{C}-\text{O}$	1028	$\nu_s\text{CH}_3$	2803
			$\nu\text{C}-\text{O}$	1050

In order to confirm the formation of the acetyl and acetate species, chemical trapping by  $\text{CH}_3\text{I}$  in large excess has been performed after the reaction of  $\text{CH}_3\text{I} + \text{CO}$  on the catalytic surface at  $180^\circ\text{C}$ . Acetone and methyl acetate are obtained in agreement with the following reactions.



This confirms the presence of acetyl and acetate species. The importance of this finding will be discussed below.

### 3.9. $\text{CH}_3\text{OH} + \text{CO}$ (Fig. 4)

During the chemisorption of  $\text{CH}_3\text{OH} + \text{CO}$  on  $\text{Rh}/\text{Pr}_6\text{O}_{11}$  at room temperature the characteristic bands of adsorbed  $\text{CO}$  and methoxy species are observed and summarized in Table 6. The attri-

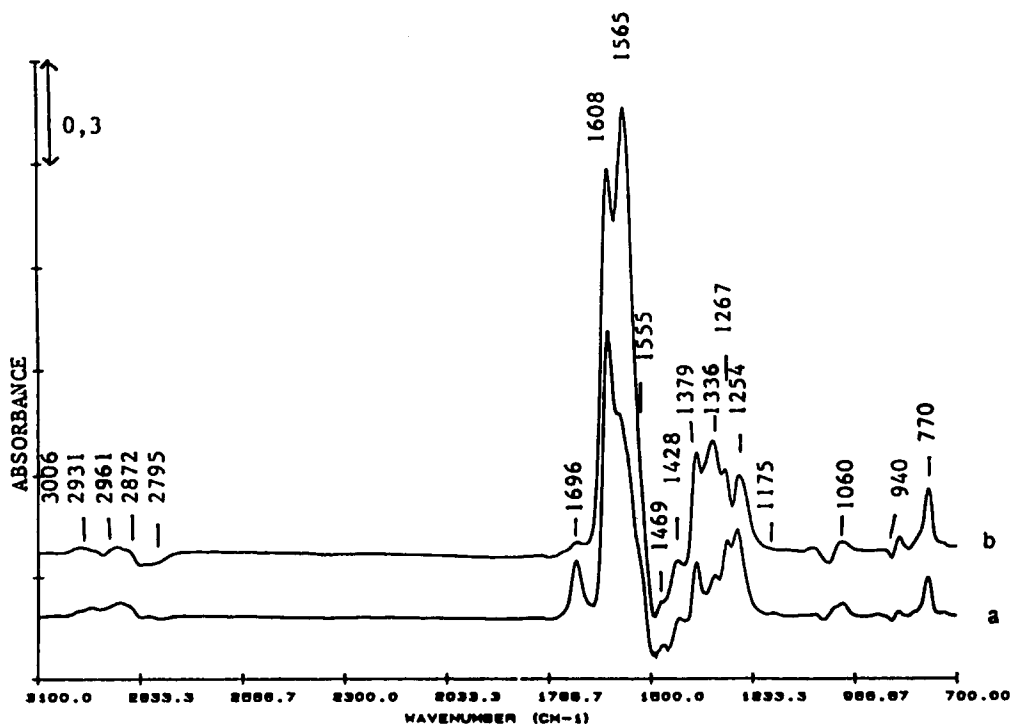


Fig. 5. FTIR spectra of methyl formate adsorbed on  $\text{Pr}_6\text{O}_{11}$  (20 mbar): (a) 60°C, (b) 180°C.

bution of bands to mono and bidentate methoxy species on  $\text{Pr}_6\text{O}_{11}$  has been made according to the results obtained by Binet et al. [36] and Li et al. [27] on  $\text{CeO}_2$ . Solymosi et al. [37] have observed the formation of methoxy species by adsorption of  $\text{CH}_3\text{OH}$  on clean  $\text{Rh}(111)$ . They observed that this species is decomposed to  $\text{CO} + \text{H}_2$  at 200–220 K. It seems therefore that the support stabilizes the methoxy species formed on the rhodium particle.

When the temperature is increased from room temperature to 120°C new features appear. The band at  $1715\text{ cm}^{-1}$  can be attributed to a C and O coordinated carbon monoxide. The other bands can be ascribed to two bidentate formate ( $\nu_a(\text{OCO})$ :  $1578$ ,  $\nu_s(\text{OCO})(\text{I})$ :  $1371$ ,  $\nu_s(\text{OCO})(\text{II})$ :  $1346$ ;  $\delta(\text{OCO})$ :  $765$ ), to an oxymethylene species ( $\delta\text{CH}_2$ :  $1478$  and  $\nu\text{CO}$   $1154\text{ cm}^{-1}$ ) and to a formyl entity ( $\nu\text{C}=\text{O}$ :  $1501$ ;  $\delta\text{CH}$ :  $1401\text{ cm}^{-1}$ ) located on the support. In the methanol adsorption, the band of linear CO is observed at  $2012\text{ cm}^{-1}$  and in presence of  $\text{CH}_3\text{OH} + \text{CO}$  at  $2050\text{ cm}^{-1}$  compared to  $2066\text{ cm}^{-1}$  with pure CO. The differences can probably be attribute to

a decrease in dipole–dipole interactions caused either by a lower CO coverage or by dilution of CO by carbonaceous residues ( $\text{CH}_3$ ,  $\text{CH}_3\text{O}$ ) from methanol decomposition.

On the support alone, the bands corresponding to mono and bidentate methoxy species are also present, together with features corresponding to formates. The oxymethylene features are not observed. No acetyl species are observed on the support alone or on  $\text{Rh}/\text{Pr}_6\text{O}_{11}$ . On the support alone unlike on  $\text{Rh}/\text{Pr}_6\text{O}_{11}$ , slight amounts of acetate are formed ( $\nu_a(\text{C}-\text{C})$ :  $96\text{ cm}^{-1}$ ,  $\delta_a(\text{CH}_3)$ :  $1445\text{ cm}^{-1}$ ,  $\nu_s(\text{CH}_3)$ :  $2926\text{ cm}^{-1}$  and  $\nu_a(\text{CH}_3)$ :  $2978$ ,  $3015\text{ cm}^{-1}$ ). This is in agreement with the results of Ichikawa and Fukushima [38] who have shown that only a minor part of ethanol or acetaldehyde formed in  $\text{CO} + \text{H}_2$  reactions incorporated  $^{13}\text{C}$  by addition of  $^{13}\text{CH}_3\text{OH}$  into the inlet gas flow.

### 3.10. Adsorption of methyl formate (Fig. 5)

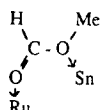
In the reactivity experiments it has been found that in the reaction  $\text{CH}_3\text{I} + \text{CH}_3\text{OH} + \text{CO} + \text{H}_2$ ,

acetic acid or methyl acetate could be produced on the support alone with no further chain growth. It is also known from the literature that acetic acid can be produced by isomerization of methyl formate [5–7]. Methyl formate has therefore been adsorbed on  $\text{Pr}_6\text{O}_{11}$  to see if acetic acid or acetate species can be formed.

At room temperature, methoxy species ( $\nu\text{CH}_3$ : 2931, Fermi resonance  $2\delta\text{CH}_3 + \nu\text{sCH}_3$ : 2872,  $\nu\text{sCH}_3$ : 2795,  $\delta\text{CH}_3$ : 1469;  $\nu\text{C-O}$ : 1060  $\text{cm}^{-1}$ ) as well as monodentate formate ( $\nu\text{a(OCO)}$ : 1608;  $\nu\text{s(OCO)}$ : 1267) and two types of bidentate formates ( $\nu\text{a(OCO)}$ : shoulder 1555;  $\nu\text{s(OCO)}$ : 1379 (I),  $\nu\text{s(OCO)}$ : 1336 and  $\delta(\text{OCO})$ : 770  $\text{cm}^{-1}$ ) and dioxymethylene species ( $\delta\text{CH}_2$ : 1469 and

$\nu\text{C-O}$ : 1175  $\text{cm}^{-1}$ ) are formed. By heating the features ascribed to methoxy and dioxymethylene species diminish, the formates are strongly increased. Bands which can be ascribed to acetate entities appear ( $\nu\text{aCH}_3$ : 3006;  $\nu\text{sCH}_3$ : 2961;  $\nu\text{s(OCO)}$ : 1428, combination between  $\delta(\text{OCO})$  and  $\rho(\text{OCO})$ : 1254 and  $\nu\text{aC-C}$  together with the intense  $\nu\text{a(OCO)}$  band at 1565  $\text{cm}^{-1}$ ).

Recently in homogeneous catalysis, the possibility of the formation and migration of methyl carbenium ion by the action of Lewis acid on methyl formate was suggested for the catalytic system  $[\text{PPh}_3\text{Pt}(\text{OAc})_2]_2^+ \text{BF}_4^-$  [39].



has been proposed by Onishi et al., [40] for the activation mode of methyl formate with a  $\text{Ru}^{\text{II}}-\text{Sn}^{\text{II}}$  cluster system. It is suggested that such a multicenter interaction may facilitate the overall rearrangement of the  $\text{CH}_3$  group (from O to C) to realize the isomerization of methyl formate to acetic acid. From our FTIR result a mechanism similar to that proposed in refs. [39] and [40] may operate on  $\text{Pr}_6\text{O}_{11}$  which is partially reduced and contains  $\text{Pr}^{4+}$  and  $\text{Pr}^{3+}$  ions which can play the role of  $\text{Ru}^{\text{II}}$  and  $\text{Sn}^{\text{II}}$  respectively.

## 4. Conclusion

It is well known that the main problem in the methanol carboxylation is the rupture of the C–O bond of  $\text{CH}_3\text{OH}$  or of  $\text{CH}_3\text{O}$  species. The results obtained in the present work show that acetate or acetic acid are not formed directly from methanol and CO on the rhodium containing catalysts. The  $\text{CH}_3$  species obtained by the reaction of  $\text{CH}_3\text{I}$  with the rhodium gives an acetyl entity which is the chain growth intermediate in acetic acid formation in agreement with the results in homogeneous catalysis [41]. However acetic acid has been shown to be formed on  $\text{Pr}_6\text{O}_{11}$  alone. In this case another mechanism must be operative. From our results in FTIR spectroscopy, it can be seen that no chain growth occurs from  $\text{CH}_3\text{I} + \text{CO}$  and that only slight amounts of acetate are formed from  $\text{CH}_3\text{OH} + \text{CO}$ . It is therefore proposed that acetic acid is formed by isomerization of methyl formate.

## 5. Unlinked References

[17]

## References

- [1] R. Schultz, (Monsanto Co.), US Pat. 3 717 670 (1973).
- [2] J.F. Knifton, Prep. Am. Chem. Soc. Div. Pet. Chem., 31 (1986) 26.
- [3] U. Dettmeier, E.I. Leupold, H. Poell, H.J. Schmidt and J. Schultz, Erdöl Kohle, Erdgas, Petrochem., 38 (1985) 59.
- [4] T.W. Dekleva and D. Forster, Adv. Catal., 34 (1986) 81.
- [5] M. Roeper, E.O. Elvevoll and M. Luetgendorf, Erdöl Kohle, Erdgas, Petrochem., 38 (1985) 38.
- [6] Halcon CD Group Inc., Neth. Pat. Appl. NL 8202 188 (1982).
- [7] D.J.M. Ray (BP Chemicals Ltd.), Eur. Pat. Appl. EP 60 695 (1982).
- [8] Agency Industrial Sciences and Technology, Jpn. Pat. JP 5,931,730 (1984).
- [9] E. Tempesti, A. Kiennemann, S. Rapagna, G. Jenner, L. Giuffre and C. Mazzocchia, It. Pat. IT 207 456 (1989).
- [10] E. Tempesti, A. Kiennemann, S. Rapagna, C. Mazzocchia and L. Giuffre, Chem. Ind., (1991) 548.
- [11] J. Lamotte, Thèse d'Etat, Caen, (1987).
- [12] R. Breault, J.P. Hindermann, A. Kiennemann and M. Laurin, Stud. Surf. Sci. Catal., 19 (1984) 489.
- [13] A.M. de Jong and J.W. Niemantsverdriet, J. Chem. Phys., 101 (1994) 10126.

- [14] J.C. Lavalley, J. Saussey, J. Lamotte, R. Breault, J.P. Hindermann and A. Kiennemann, *J. Phys. Chem.*, 94 (1990) 5941.
- [15] D. Demri, J.P. Hindermann, A. Kiennemann and C. Mazzocchia, *Catal. Lett.*, 23 (1994) 227.
- [16] B.J. Kip and E.G.F. Hermans, in M.J. Philipps and M. Terman (Eds.), *Proc. 9th Int. Congr. Catal. (Calgary)*, Vol. II, 1988, p. 821.
- [17] J.P. Hindermann, G.J. Hutchings and A. Kiennemann, *Catal. Rev. Sci. Eng.*, 35 (1993) 1 and refs. therein.
- [18] H.J.F. van't Blik, J.B.D.A. van Zon, T. Huizinga, J.C. Vis, D.C. Koningsberger and R. Prins, *J. Am. Chem. Soc.* 107 (1985) 3139.
- [19] F. Solymosi and M. Pasztor, *J. Phys. Chem.*, 89 (1985) 4789.
- [20] J.T. Yates, Jr., T.M. Duncan, S.D. Worley and R.W. Vaughan, *J. Chem. Phys.*, 70 (1979) 1219.
- [21] H.J.F. van't Blik, J.B.D.A. van Zon, D.C. Koningsberger and R. Prins, *J. Mol. Catal.*, 25 (1984) 379.
- [22] F. Solymosi and M. Pasztor, *J. Phys. Chem.* 90 (1986) 5312.
- [23] F. Solymosi and H. Knözinger, *J. Chem. Soc. Faraday Trans* 86 (1990) 389.
- [24] M. Ichikawa, P.E. Hoffmann and A. Fukuoka, *J. Chem. Soc. Chem. Commun.*, (1985) 1395.
- [25] D. Demri, L. Chateau, J.P. Hindermann, A. Kiennemann and M.M. Bettahar, *J. Mol. Catal. A*, in press.
- [26] G.J. Millar, C.H. Rochester and K.C. Waugh, *J. Chem. Soc., Faraday Trans*, 87 (1991) 1491.
- [27] C. Li, K. Domen, K.I. Maruya and T. Onishi, *J. Catal.*, 125 (1990) 445.
- [28] G. Busca, J. Lamotte, J.C. Lavalley and V. Lorenzelli, *J. Am. Chem. Soc.*, 109 (1987) 5197.
- [29] J. Saussey, T. Rais and J.C. Lavalley, *Bull. Soc. Chim. Fr.*, (1985) 305.
- [30] H. Hattori and G.W. Wang, *Proc. 8th Int. Congr. Catal. (Berlin)*, Vol. III, Verlag Chemie, Weinheim, 1984, p. 219.
- [31] B.A. Sexton, *Chem. Phys. Lett.*, 65 (1979) 469.
- [32] K. Ito and H.J. Bernstein, *Can. J. Chem.*, 34 (1956) 170.
- [33] D. Demri, J.P. Hindermann, C. Diagne and A. Kiennemann, *J. Chem. Soc., Faraday Trans. 1*, 90 (1994) 501.
- [34] M.A. Henderson, Y. Zhou and J.M. White, *J. Am. Chem. Soc.*, 111 (1989) 1185.
- [35] W. Hieber, G. Braun and W. Beck, *Chem. Ber.*, 93 (1960) 901.
- [36] C. Binet, A. Jadi and J.C. Lavalley, *J. Chim. Phys.*, 89 (1992) 1441.
- [37] F. Solymosi, A. Berko and T.I. Tarnoczi, *Surf. Sci.*, 141 (1984) 553.
- [38] M. Ichikawa and T. Fukushima, *J. Chem. Soc., Chem. Commun.*, (1985) 321.
- [39] N. Yu Kositsyna and I.I. Moiseev, *Kinet. Catal.* 32 (1991) 985.
- [40] T. Onishi, T. Suzuki, T. Yamakawa and S. Shinoda, *J. Mol. Catal.*, 84 (1993) 51.
- [41] D. Forster, *Adv. Organomet. Chem.*, 17 (1979) 255.